HIGH-RESOLUTION LOCAL-AREA DIGITAL ELEVATION MODELS AND DERIVED PRODUCTS FOR MERCURY FROM MESSENGER IMAGES. Madeleine R. Manheim[1], Megan R. Henriksen[1], Mark S. Robinson[1], and the MESSENGER Team, [1]School of Earth and Space Exploration, Arizona State University, 1100 South Cady Mall, Tempe, AZ 85287, mmanheim@ser.asu.edu.

Introduction: The Mercury Dual Imaging System (MDIS) on the MErcury Surface, Space ENvironment, GEochemistry, and Ranging (MESSENGER) spacecraft provided global images of Mercury's surface. MDIS consisted of two cameras: a monochrome narrow-angle camera (NAC) and a multispectral wide-angle camera (WAC) [1]. Although MDIS was not designed as a stereo camera, off-nadir observations acquired at different times resulted in near-global stereo coverage and enabled the creation of digital elevation models (DEMs) [1]. Low altitude stereo sequences acquired later in the mission allow the creation of local area DTMs with spatial scales more than 8x better than the global product [2]. The local DEMs were computed from NAC images with Mercury Laser Altimeter (MLA) profiles serving as a geodetic reference frame [3]. WAC stereo images controlled to MLA profiles bridged gaps in coverage or provided control when no MLA tracks passed through the NAC stereo coverage area. Previously, MDIS DEMs of comparable resolution were created with the AMES stereo pipeline [4].

Mercury Dual Imaging System. The NAC was a 1.5° field-of-view (FOV) off-axis reflector, providing images with a pixel scale of 5.1 m at an altitude of 200 km. The WAC was a four-element refractor with a 10.5° FOV and 12-color filter wheel, providing images with a pixel scale of 35.8 m at an altitude of 200 km. Each camera had an identical 1,024 x 1,024 charge-coupled device (CCD) detector [1].

Mercury Laser Altimeter. MLA was a time-of-flight altimeter that used pulse detection and pulse-edge timing to precisely determine the range from the spacecraft to the surface [3]. MLA observations were available only for latitudes between 90°N and 18°S due to MESSENGER's highly eccentric orbit and periapsis at high northern latitudes, with the measurements' density decreasing with latitude. MLA measurements had a radial precision of < 1 m and a radial accuracy of < 20 m with respect to Mercury's center of mass [5].

Methodology: High-resolution regional DEM processing was completed at Arizona State University using a combination of Integrated Software for Imagers and Spectrometers (ISIS) and SOCET SET from BAE Systems [6].

Stereo Image Selection. NAC images used for DEM production range in pixel scale from 5 m to 170 m, and image illumination conditions and spacecraft geometries vary greatly. The set of images covering a desired region was first sorted to ensure optimal lighting conditions and resolution [7]. From these images, acceptable stereo pairs were identified on the basis of common surface coverage, resolution ratio, stereo strength (parallax/height ratio), and illumination compatibility [7].

Pre-Processing. The selected images were ingested into ISIS, radiometrically calibrated, and initialized with orientation parameters stored in SPICE kernels. These parameters were converted to a format compatible with SOCET SET 5.6, and, along with the images, imported into SOCET SET [6].

Relative Orientation. Before controlling the images to the geodetically accurate MLA tracks, each image was corrected for relative orientation to the other images in the stereo model. All overlapping images were linked by a set of ~9 "tie" points, which were found by matching pixels between images and then aligned using a multi-sensor triangulation algorithm [8,9]. Our target root mean square (RMS) error was <0.5 pixels.

Absolute Orientation. The bundle-adjusted NAC images were manually controlled to the MLA profiles by identifying points along individual tracks and visually identifying their corresponding locations in the images, creating ground points. These ground points, specifying exact coordinates for given pixel locations in an image, were then included in a final bundle adjustment to triangulate absolute orientation of the images. The RMS errors in latitude, longitude, and elevation were considered acceptable within the accuracies of the MLA profiles. For NAC images with insufficient MLA coverage, overlapping WAC images were tied to the NACs and then controlled to MLA to provide indirect control.

DEM Extraction. The areas of image overlap calculated by the off-axis sensor model are not sufficiently precise to be used as a basis for extracting stereo. As a work-around, a cubic rational polynomial (CRP) approximation of the sensor model was generated for each controlled image; these approximations have residual errors less than 0.01 pixels. The CRP images were then used with the Next Generation Automatic Terrain Extraction (NGATE) program in SOCET SET to create a DEM at a pixel scale a factor of 3 greater than the largest pixel scale of an image in a stereo pair [10,11].

Orthophoto Generation. The final DEM was used to orthorectify the original NAC images, allowing for the creation of orthophotos free of distortion (within the limits of the DTM accuracy) from topography and camera viewing angle [12]. Orthophotos were generated at both the DEM resolution and the native image pixel scale.

Planetary Data System (PDS) Archive Products. In addition to the DEM, a confidence map and orthophotos of each image in the stereo pair are available at both the pixel scale of the DEM and at the largest native pixel scale from the stereo pair (PDS IMG format). A terrain shaded-relief map, a color shaded-relief map, a slope map, and corresponding legends are also provided at the pixel scale of the DEM in the EXTRAS directory of the PDS in GeoTIFF format, as well as a 32-bit GeoTIFF of the DEM. These derived GeoTIFF products were created using the Geospatial Data Abstraction Library (GDAL) [13]. For sites where multiple stereo pairs were used to build up coverage, the overlapping products were mosaicked and released in addition to all the individual products (Fig. 1).

Uncertainty Analysis: Qualitative and quantitative error analyses were performed for each DEM. Measures of accuracy for the nine sites produced are summarized in Table 1.

Linear Error. SOCET SET calculates precision as relative error at a 90% confidence level [8,11]. Vertical precision is reported as relative linear error and is expected to be less than the pixel scale of the DEM (Table 1)[14]. The horizontal precision of the DEM is equal to the pixel scale of the DEM, as pixel scale is consistently greater than the circular (or horizontal) error at 90%, as reported by SOCET SET [9,12].

Offsets from MLA. At every point that MLA tracks directly crossed the DEM, elevation offsets were calculated and the mean and standard deviation of these offsets were evaluated. If no co-located tracks were available, offsets were reported from the MLA controlled WAC DEMs used to control the NAC DEMs. Some DEMs in the southern hemisphere had no MLA coverage; these products were not absolutely controlled and report only relative precision. We would like the measured differences between the DEMs and MLA tracks to be <20 m (the radial accuracy of MLA points) [5]. However, despite ongoing refinement of both our error analysis and DEM processing methods, consistently obtaining this level of accuracy remains challenging; the seven DEMs we controlled to MLA had an average mean offset of -50.7 m, indicating that their absolute elevations were generally too high. In all but one case, we were able to achieve mean offsets less than the pixel scale of the DEM (Table 1).

Product Summary: Nine sites consisting of 57 stereo pairs are currently complete (Table 1). The MESSENGER project released these DEMs to the public through the PDS in December 2016 (available at http://bit.ly/2lMXDnj).

References: [1] Hawkins, S. E., III et al. (2007) *Space Sci. Rev., 131,* 247-338. [2] Becker, K. J. et al. (2016) *LPS, 47,* Abs. 2959. [3] Cavanaugh, J. F. et al. (2007) *Space Sci. Rev., 131,* 451-497. [4] Fassett, C. I. (2016) *Planet. Space Sci., 134,* 19-28. [5] Zuber, M. T. et al. (2012) *Science, 336,* 217-220. [6] Anderson, J. A. et al. (2004) *LPS, 35*, Abs. 2039. [7] Becker, K. J. et al. (2015) *LPS, 46,* Abs. 2703. [8] Förstner, W. et al. (2013) *Manual of Photogrammetry (6th ed.)*, 785-955. [9] BAE Systems (2011) *SOCET SET User's Manual, v*. 5.6. [10] BAE Systems (2007) *NGATE*. White Paper. [11] Zhang, B. (2006) *ASPRS,* p. 12. [12] Miller, S. et al. (2013) *Manual of Photogrammetry (6th ed.)*, 1009-1043. [13] Warmerdam, F. (2008) *Open Source Approaches in Spatial Data Handling*, 87-108. [14] Henriksen, M. R. et al. (2017) *Icarus, 283,* 122-137.

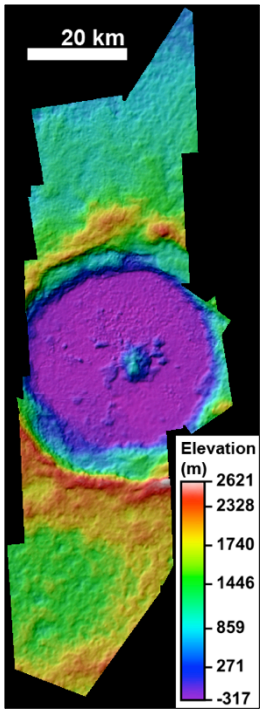

Fig. 1. Color shaded-relief map of Sander crater DEM mosaic, derived from 21 images forming 36 stereo pairs.

Table 1. Summary of MDIS NAC DEMs produced in this study.

Site Name	No. of Stereo Pairs	Center Latitude, Longitude (°N, °E)	Mosaic Pixel Scale (m)	Relative Linear Error (m)	MLA Mean Offset (m)	MLA Standard Deviation (m)
Catullus Crater	1	21.88°, 292.5°	84	84	-255	188
Cunningham Crater	9	30.40°, 157.0°	105	85	2	58
Degas Crater	1	36.86°, 232.6°	97	70	-1	109
Hynek Scarp*	1	-31.16°, 82.5°	500	383	-	-
Kertesz Crater	2	31.45°, 146.3°	120	98	-9	51
Kuiper Crater	1	-11.3°, 329.1°	270	161	-	-
Paramour Rupes	3	-5.07°, 145.1°	450	261	-5	185
Raditladi Hollows	3	15.20°, 120.2°	180	137	-44	52
Sander Crater	36	42.50°, 154.7°	162	70	-44	65

**Unofficial name.*